Are Transport Anomalies in "Electron Waveguides" Classical?

M. L. Roukes, A. Scherer, and B. P. Van der Gaag
Bellcore, Red Bank, New Jersey 07701
(Received 27 November 1989)

We test the implicit prediction of a recent classical model that transport anomalies in ballistic multiprobe conductors—the last plateau, quenching, and the negative bend resistance—should scale with Fermi momentum, p_F. Data from junctions defined by *adiabatic* lateral potentials (having corners with radii of curvature $r_J > \hbar/p_F$) qualitatively scale classically; departures observed are attributed to momentum-memory loss from random scattering. With more *abrupt* (square cornered) junctions, however, nonclassical p_F dependence emerges.

PACS numbers: 72.20.My, 73.40.Kp, 73.50.Jt

In a narrow ballistic wire the interpretation of an electrical measurement is complicated because resistance is *nonlocal*. Usually, a four-probe electrical measurement allows sampling of specific portions of the voltage drop along the path of the current. In multiterminal ballistic conductors, however, voltages developed at probes are not solely determined by the properties of the current-carrying region between them. Despite these ambiguities, narrow probes have been used to "sample" narrow wires, initially with the hope of exploring the physics intrinsic to quasi-one-dimensional (Q1D) conductors. Unexpected features at low magnetic fields have been revealed—a peak at finite B in the magnetoresistance, $R(B)$;[1] anomalies in the Hall resistance, R_H, referred to as quenching and the last plateau;[1] and bend resistances, R_B,[2] and ΔR_s.[3] Except for the peak in $R(B)$,[4] experiments and theory now indicate that these unusual features originate from *scattering at the junctions* connecting probes and wires, rather than from intrinsic Q1D properties of the wires themselves.[5]

Several numerical studies have focused on the quantum mechanics of junction scattering.[6-10] These have led to explanations for the observed anomalies couched in terms of transport in the few-subband limit, where the *mode-selective* properties of junction scattering become important.[5(b)] Recently, however, Beenakker and van Houten,[11] through *classical* electron-trajectory calculations, have produced magnetoresistance curves bearing features remarkably similar to those observed in experiments. This is surprising and counter to widely held assumptions (including ours), since it suggests that the few-mode aspect of the experiments is *not* essential to the development of these anomalies.

In this Letter we test this simple classical model. Perhaps its most striking feature is that it generates *universal* magnetoresistance curves. Their axes are normalized by two characteristic quantities: *resistance* by $R_0 = (\hbar\pi/e)^2(1/p_F W)$, the ballistic sheet resistivity for a 2D "wire" of width W (the analog of a Knudsen resistance for 2D electrons);[12] and *magnetic field* by $B_0 = p_F/eW$, the field at which the cyclotron radius, r_c, equals W. Both quantities are basically classical; $\hbar$ appears solely through introduction of Fermi-Dirac statistics. The detailed *shapes* of these normalized curves are determined by junction geometry alone—in the simplest case of a round-cornered junction and square-well potentials this involves only the dimensionless variable, $\hat{r} = r_J/W$. Here, r_J is the radius of curvature at the corners. This suggests that R_0 and B_0 can be experimentally "tuned" in two different ways. The first involves *size:* At fixed $\hat{r}$ and electron density, n_s [and, hence, fixed $p_F = (2\pi\hbar^2 n_s)^{1/2}$],[13] magnetoresistance data from samples of arbitrary size ($\propto W$) should *scale* onto one universal curve. The second involves *momentum:* Experimental data at different p_F from a *single* sample of fixed geometry should also scale onto a universal curve. In this situation each anomaly should evolve with p_F in a *monotonic* and completely prescribed manner. Testing *size* scaling is difficult since it requires many ballistic samples of different sizes, all with identical $\hat{r}$. Below we investigate the second, more readily accessible, type of one-parameter scaling.

Our investigations are carried out in structures specifically designed and fabricated to test classical p_F scaling. A GaAs/AlGaAs two-dimensional electron-gas heterojunction ($\mu = 0.98\times10^6$ cm^2/Vsec, $n_s = 3.0\times10^{11}$ cm^{-2}) is patterned by electron-beam lithography and very low-energy ion exposure into miniature wires and junctions.[14] Application of a bias potential, V_g, to a self-aligned gate alters n_s in these narrow conductors.[5(a)] Our devices are unique in that their conducting geometry, determined by lithography, remains essentially fixed while n_s and, hence, p_F, is varied.[5(c)] Evidence for this is obtained from *each* junction by tracking magnetic depopulation of the Q1D magnetoelectric levels[15] via the quantum Hall effect for each value of V_g.[16] (An example is displayed in Fig. 1.) This property, also confirmed through other experiments,[4,14] is essential for attempting comparisons with theories which do not include self-consistent potentials. It has not been obtained with the gated ballistic devices used in other recent studies.

Using these junctions we follow the evolution of each transport anomaly with p_F ($\propto \sqrt{n_s}$) and compare the results against the predicted scaling. Several hundred miniature samples with $W \sim 0.25$ μm were fabricated; twenty-four of these have been carefully studied. Con-

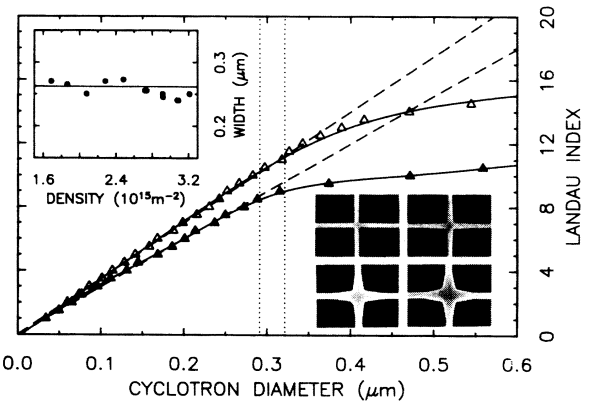

FIG. 1. Depopulation diagram obtained from the quantum Hall effect at a junction for two values of V_g, -100 mV (solid triangles) and $+250$ mV (open triangles) where ~ 11 and ~ 15 modes, respectively, are occupied at $B=0$. From the high-B linear portion of the data on the left, n_s is extracted (dashed lines). This is used to transform abscissas from units of $1/B$ to those of cyclotron diameter, $(8\pi\hbar^2 n_s)^{1/2}/eB$. Over the range of gate voltages employed, the deduced electrical widths, w_{el} (dotted lines), change by only $\sim 10\%$. Top inset: Here, w_{el}, determined more conventionally from quantum oscillations in the magnetoresistance of 6-μm-long wire segments between junctions, shows negligible n_s dependence. Bottom inset: Electron micrographs of straight and flared junctions connecting $W \sim 0.25$ μm wires.

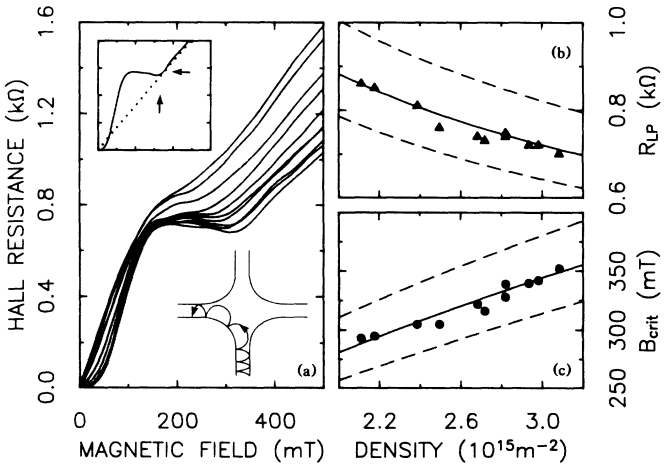

FIG. 2. (a) Evolution of the last plateau with varying n_s for junction (f). Top inset: Two characteristics of this anomaly are tracked with n_s: R_{LP}, the resistance on the plateau, and B_{crit}, its intersection with the Hall effect in the diffusive limit, $R_H^{(d)} = B/n_s e$ (dotted line). Bottom inset: A guiding trajectory. (b),(c) Data for R_{LP} and B_{crit} (points) follow predicted curves only for assumed widths $W = 410$ and 520 nm (solid lines), respectively, almost twice the measured value. Dashed lines are predictions for widths ± 50 nm about these values.

trolled rounding of the junction corners was achieved lithographically (Fig. 1).[17] For each junction of this select group, 11–16 magnetoresistance traces (at different values of n_s) were obtained at 1.8 K, without illumination, for two separate probe configurations yielding R_H and R_B. The data presented here—from three specific junctions referred to as (s), (f), and (gf), to describe their *straight, flared,* and *grossly flared* junction corners, respectively[18]—are representative of trends observed in the complete set of devices characterized.

As described below, p_F scaling is only observed in several specific situations. We analyze our results using an approach analogous to ray tracing in geometric optics. This provides explanations for the anomalies based on four classical trajectories: the *guiding,*[11] *scrambling,*[11] *rebound,*[19] and *collimation*[20] trajectories. These are specific paths taken by electrons between the time of their injection into the junction from one lead, and their ultimate collection by another. They can involve numerous reflections at the boundaries and long effective path lengths within the junction. In this work, we shall explicitly assume electrons can be scattered from these well-defined trajectories through diffuse boundary scattering and bulk mechanisms.[4,21] Viewed from this perspective, our results elucidate the important role of the *finite momentum memory* of electrons in real samples.

We turn first to the anomalies in R_H. Büttiker's model[22] describes the development of R_H at a ballistic four-terminal junction. In a symmetric cross at $B=0$, transmission probabilities from the injection (*current*) probe into the right and left (*voltage*) probes, T_R and T_L, are equal. At finite B, however, the Lorentz force, $\mathbf{F}_L = -e\mathbf{v}\times\mathbf{B}$, enhances transmission into one voltage probe at the expense of the other; $T_L(B) > T_R(B)$. This asymmetry alters the relative chemical potentials of reservoirs attached to these leads, thereby generating a Hall effect, $R_H \propto T_L - T_R$. In a junction with rounded corners, *guiding* trajectories [Fig. 2(a), inset] can increase T_L at low B, prematurely elevating R_H to R_0. This "saturation" of R_H has been advanced as the mechanism inducing the last plateau.[11] Data from junction (f) at high densities show a fully developed plateau beginning at 200 mT [Fig. 2(a)], but this decays away as n_s is reduced. Although its disappearance at low n_s is counter to the classical prediction, two characteristic features of the plateau (described in the caption), R_{LP} and B_{crit}, evolve roughly as predicted [Figs. 2(b) and 2(c)]. Guiding involves relatively few boundary reflections and short path lengths, thus momentum-memory loss during junction traversal should be minimal. This qualitative scaling of R_{LP} and B_{crit} is observed for all junctions of this study. Quantitative agreement with the predicted curves, $B_{crit} = 2B_0$ and $R_{LP} = R_0$, however, is obtained only for assumed values of W roughly twice that measured by depopulation. This is well beyond the estimated experimental uncertainty ($< \pm 50$ nm).

In a ballistic cross junction, the Hall slope near $B=0$ can be quenched[1] or negative.[5(a),19] Quenching has been ascribed to *scrambling* trajectories which suppress the transmission asymmetry $[T_L(B) > T_R(B)]$ expected at

finite B.[11] This suppression is argued to result from the temporary trapping of electrons into complex, multiply scattered paths within the junction [Fig. 3(b), inset]; it is supposed that emerging electrons have equal probability of transmission into the side probes. Figure 3(a) depicts the n_s evolution of R_H near zero field for junction (f). Strong suppression of R_H at low B is seen for higher n_s. The simple model predicts that *all* Hall slopes, irrespective of junction rounding, should be p_F *independent* when normalized by the Hall slope in the diffusive limit, $dR_H^{(d)}/dB = 1/n_s e$. Accordingly, in Fig. 3(b) we plot the normalized low-B slope against n_s. For junction (f) no region of p_F independence is evident; instead, the slope rises monotonically with reduced n_s to the diffusive value (~ 1). This suggests that complete scrambling necessitates longer momentum memories than available, even at high n_s where the transport mean free path, l_0, is quite long (~ 9 μm). Note that the full Hall effect $R_H = B/n_s e$ will always be recovered in the diffusive limit entered at low n_s where unscreened potential fluctuations reduce l_0.

In this same region the more flared junction (gf) displays negative R_H [Fig. 3(c)]. The negative slope scales with p_F; a constant, negative (normalized) slope is observed for $n_s > 2.8\times 10^{11}$ cm^{-2} [Fig. 3(d)]. Negative R_H has been argued to arise from *rebounding* of electrons from the rounded corners of a very flared junction [Fig. 3(d), inset].[19] This enhances T_R at low B when, otherwise, F_L would cause $T_L > T_R$. This observed scaling agrees with our expectation that rebound trajectories involve relatively short path lengths, few boundary collisions and, thus, minimal **p** randomization during junction traversal.

A negative bend resistance R_B (Ref. 2) is observed with the lead configuration shown in Fig. 4(d) (inset).[23] Ballistic transferral of carriers into the "wrong" (i.e., forward) lead generate this negative four-probe resistance; a positive value is recovered in the diffusive limit. Collimation trajectories [Fig. 4(b), inset] are important for the development of this anomaly. These increase forward transmission while reducing that into the side probes: $T_F > T_L, T_R$.[10] Collimation thus enhances R_B —other trajectories besides the obvious, direct "straight-shot" paths can contribute to T_F.[4(b),21] We display the n_s dependence of R_B at $B=0$ for junctions (f) and (gf) in Figs. 4(a), 4(b) and 4(c), 4(d), respectively. Although scaling predicts that $R_B(0)/R_0$ should be p_F independent, this is not observed. Instead, all junctions measured in this work display an unexpected monotonic *increase* in $|R_B(0)/R_0|$ with *increasing* n_s. This behavior is also contrary to that predicted by mode-selection arguments.[3,5(b),8-10] Collimated electrons follow long, complex trajectories susceptible to random scattering. As density is reduced, their contributions to R_B are progressively eliminated as l_0 shrinks. The observed lack of scaling for $R_B(0)$ and its dependence upon junction geometry [Figs. 4(b) and 4(d)] is consistent with this picture.[4(b),21]

Finally, in Figs. 3(e) and 3(f) we display R_H and its normalized slope for junction (s) which has extremely sharp corners.[18] Striking *nonmonotonic* density dependence is evident, clearly different than monotonic trends displayed by the flared junctions.[24] This is reminiscent of the oscillatory Hall slope predicted by quantum-mechanical simulations and attributed to resonances at junctions.[5(d),6,7,25] Here, thermal averaging and the ap-

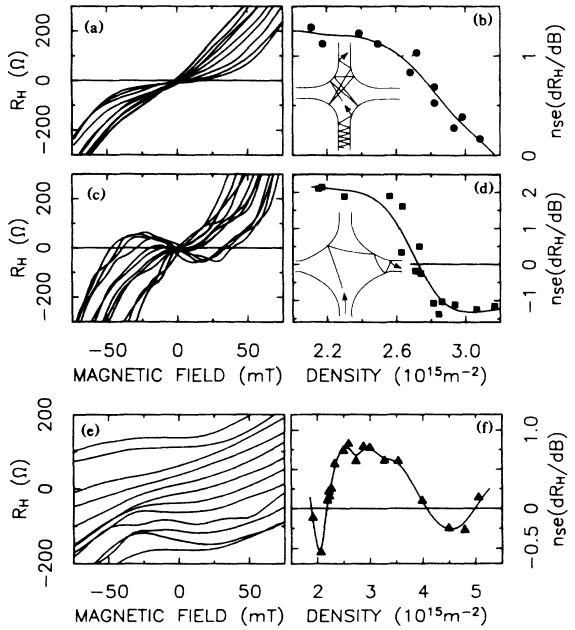

FIG. 3. Hall anomalies at low B and their density dependence: (a),(b) for the flared junction; (c),(d) for the grossly flared junction; and (e),(f) for the straight junction. In (e), the traces from junction (s) are offset to clearly display its *reentrant* quenching behavior. The curvature of relevant trajectories (shown as insets), when compared to Fig. 2, reflects the lower fields involved here.

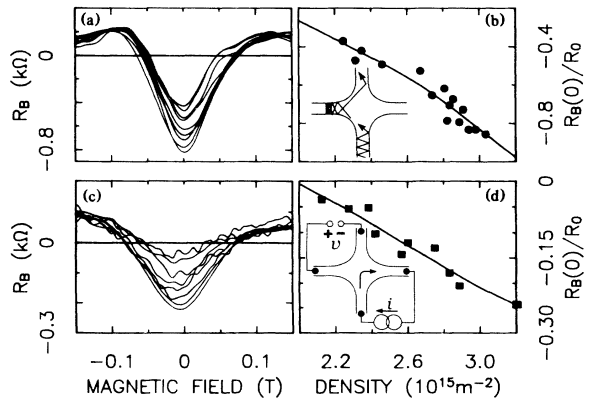

FIG. 4. The bend resistance R_B at low B and its density dependence: (a),(b) for the flared junction; (c),(d) for the grossly flared junction. Insets: A collimation trajectory and the probe configuration used to measure R_B.

proximately four subbands between Hall-slope minima probably preclude such explanations. Similar behavior has been observed in four sharp-cornered junctions in which r_J is comparable to the electron wavelength, $\lambda_F \sim 2\pi/k_F$. For these abrupt junctions, electron diffraction should become important—here, as in geometric optics, ray tracing cannot explain *interference* phenomena.

Our results suggest that the transport anomalies observed to date in ballistic junctions are *classical size effects.*[26] Scaling predicted by the simple model is qualitatively confirmed for anomalies involving the least complicated electron trajectories. Refinements to this model, to properly account for the electron's finite momentum memory in real samples, appear essential for explaining the observed departures from scaling. The data suggest the simple model fails most drastically for phenomena developed only after many boundary reflections and traversal of long paths within the junction; these are most susceptible to **p** randomization.

In retrospect, the simple model's results are not totally unexpected—recent quantum-mechanical simulations agree with experiments only when altered to include extremely flared model potentials, many occupied modes, and thermal averaging;[10] similarly, trajectory diagrams successfully explain the geometry dependence of Hall anomalies in multimode, round-cornered (i.e., adiabatic) junctions[19]—these aspects favor *classical* physics. Taking a larger view, we expect ray tracing is valid for all ballistic devices having adiabatic lateral potentials and many occupied modes. As suggested by our preliminary data from devices with sharp corners, this should break down for very small junctions where abrupt potentials and occupation of only a few modes cause nonclassical behavior to emerge. It now seems clear that this *quantum* regime in ballistic microstructures remains, still, largely *unexplored.*

We thank S. J. Allen, Jr., H. U. Baranger, C. W. J. Beenakker, M. Büttiker, A. Del Vescovo, G. Kirczenow, F. M. Peeters, T. J. Thornton, and J. M. Worlock for illuminating discussions.

[1]M. L. Roukes *et al.*, Phys. Rev. Lett. **59**, 3011 (1987).

[2]Y. Takagaki *et al.*, Solid State Commun. **68**, 1051 (1988).

[3]G. Timp *et al.*, Phys. Rev. Lett. **60**, 2081 (1988).

[4]We attribute this low-B peak to *classical* boundary scattering: (a) T. J. Thornton, M. L. Roukes, A. Scherer, and B. P. Van der Gaag, Phys. Rev. Lett. **63**, 2128 (1989); (b) M. L. Roukes, T. J. Thornton, A. Scherer, and B. P. Van der Gaag, in *Electronic Properties of Multilayers and Low-Dimensional Semiconductor Structures,* edited by J. M. Chamberlain, L. Eaves, and J. C. Portal (Plenum, London, 1990).

[5](a) M. L. Roukes *et al.*, in *Science and Engineering of 1- and 0-Dimensional Semiconductors,* edited by S. P. Beaumont and C. M. Sotomayor-Torres (Plenum, New York, 1990), and references therein; (b) see, e.g., H. U. Baranger and A. D. Stone, *ibid.*; (c) T. J. Thornton, M. L. Roukes, A. Scherer, and B. P. Van der Gaag, *ibid.*; (d) F. M. Peeters, *ibid.*

[6]D. G. Ravenhall, H. W. Wyld, and R. L. Schult, Phys. Rev. Lett. **62**, 1780 (1989); Phys. Rev. B **39**, 5476 (1989).

[7]G. Kirczenow, Phys. Rev. Lett. **62**, 1920 (1989); **62**, 2993 (1989).

[8]G. Kirczenow, Solid State Commun. **71**, 469 (1989).

[9]Y. Avishai and Y. B. Band, Phys. Rev. Lett. **62**, 2527 (1989).

[10]H. U. Baranger and A. D. Stone, Phys. Rev. Lett. **63**, 414 (1989).

[11]C. W. J. Beenakker and H. van Houten, Phys. Rev. Lett. **63**, 1857 (1989).

[12]Yu. V. Sharvin, Pis'ma Zh. Eksp. Teor. Fiz. **48**, 984 (1965) [Sov. Phys. JETP **21**, 655 (1965)].

[13]This relation holds when the number of occupied Q1D modes, N_{occ}, is large. In these experiments $N_{occ} \sim 5$–15 (see Fig. 1).

[14]A. Scherer and M. L. Roukes, Appl. Phys. Lett. **55**, 377 (1989).

[15]K. F. Berggren *et al.*, Phys. Rev. Lett. **57**, 1769 (1986).

[16]The conducting width, w_{el}, can only be *accurately* obtained from depopulation data if the exact shape of the confining potential is known. Here, the important point is that the extracted value of w_{el} *remains constant* as n_s is varied.

[17]A lower limit to r_J is imposed by edge depletion (see Ref. 14). We estimate that our highly optimized method can yield $4_J^{(min)} \sim 20$ nm, but for the *flared* junctions of this study we *intentionally* (greatly) exceed this minimum.

[18]We estimate that $r_J/W \sim 0.1$, 0.5, and 2 for junctions (s), (f), and (gf), respectively, but stress these are only approximate average values.

[19]C. J. B. Ford *et al.*, Phys. Rev. Lett. **62**, 2724 (1989).

[20]C. W. J. Beenakker and H. van Houten, Phys. Rev. B **39**, 10445 (1989).

[21]M. L. Roukes, O. Alerhand, A. Scherer, and B. P. Van der Gaag (unpublished).

[22]M. Büttiker, Phys. Rev. Lett. **57**, 1761 (1986); Phys. Rev. B **38**, 9375 (1988).

[23]R_B is one example of a larger class of *transfer* resistances. As shown in Refs. 4(b) and 21, these are *generalized* resistances—voltage probes may be placed outside the net path of the current. Timp *et al.* (Ref. 3) observed an increase in the (conventional) resistance, ΔR_s, induced by a bend in the current path. Although measurement of ΔR_s involves a minimum of two junctions, in Ref. 21 it is shown to be closely related to an idealized resistance difference involving a *single* cross junction: $\Delta R_s \sim R_{12,14} - R_{13,14}$. [Here, the first (second) pair of indices represent the current (voltage) probes, and lead numbering increases counterclockwise.] For a symmetric cross junction Büttiker's model yields $R_{12,14} - R_{13,14} = -R_B$ [G. Kirczenow (private communication)]. This suggests that ΔR_s, like R_B, originates classically.

[24]Classical "deterministic chaos" predicted to arise in *flared* junctions might also lead to nonmonotonic behavior. These effects, however, involve many specular reflections and long path lengths within the junction. We expect that momentum-memory loss, shown in the present work to limit the development of transport anomalies, is important in this context as well.

[25]F. M. Peeters, Superlattices Microstruct. **6**, 217 (1989).

[26]We expect that classical descriptions of the anomalies remain essentially correct, even when nonclassical effects (e.g., mode-selective injection into multimode junctions and quantum interference) begin to weakly "modulate" them.

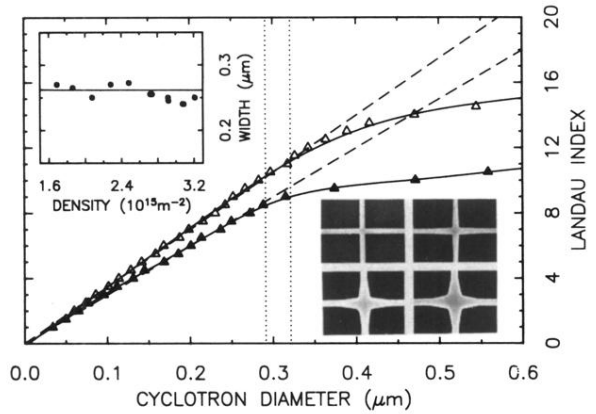

FIG. 1. Depopulation diagram obtained from the quantum Hall effect at a junction for two values of V_g, -100 mV (solid triangles) and $+250$ mV (open triangles) where ~ 11 and ~ 15 modes, respectively, are occupied at $B=0$. From the high-B linear portion of the data on the left, n_s is extracted (dashed lines). This is used to transform abscissas from units of $1/B$ to those of cyclotron diameter, $(8\pi\hbar^2 n_s)^{1/2}/eB$. Over the range of gate voltages employed, the deduced electrical widths, w_{el} (dotted lines), change by only $\sim 10\%$. Top inset: Here, w_{el}, determined more conventionally from quantum oscillations in the magnetoresistance of 6-μm-long wire segments between junctions, shows negligible n_s dependence. Bottom inset: Electron micrographs of straight and flared junctions connecting $W \sim 0.25$ μm wires.